THE ASTROPHYSICAL JOURNAL, 489:758–765, 1997 November 10

PROBING THE PHOTODISSOCIATION REGION TOWARD HD 200775

S. R. FEDERMAN[1,2] AND D. C. KNAUTH
Department of Physics and Astronomy, University of Toledo, Toledo, OH 43606
DAVID L. LAMBERT
Department of Astronomy, University of Texas, RLM 15.308, Austin, TX 78712-1083
AND
B-G ANDERSSON[1,2]
Jet Propulsion Laboratory, California Institute of Technology, 4800 Oak Grove Drive, Pasadena, CA 91109
Received 1997 January 24; accepted 1997 June 24

ABSTRACT

The illuminating source of the photodissociation region associated with the reflection nebula NGC 7023 is HD 200775. We probed the foreground atomic and molecular material through diagnostics observed in absorption against the background star. Ground-based measurements of Na I, K I, and Ca II and of the molecules CH, CH^+, C_2, and CN were analyzed in order to extract the physical conditions for this material. In particular, estimates for gas density, gas temperature, and the flux of ultraviolet radiation were derived and compared with information obtained from maps of radio emission. The foreground material has lower density than the other portions of the photodissociation region; the observed excitation of C_2, the observed column of C_2, and the columns of neutral sodium and potassium are reproduced when the extinction curve derived for this line of sight is adopted. Future models of the NGC 7023 nebula should include the effects associated with this extinction curve. The observed CN column density is larger than our predicted amount; an additional contribution from the background molecular cloud is inferred.

Subject headings: ISM: abundances — ISM: individual (NGC 7023) — ISM: molecules — reflection nebulae — stars: individual (HD 200775)

1. INTRODUCTION

The illuminating source of a reflection nebula affects the surrounding gas in a number of ways. For instance, although few ionizing photons are available to create an H II region, photons with energies between the Lyman limit and about 1100 Å produce a photodissociation region around the star, a zone in which H_2 and CO are destroyed through absorption of ultraviolet photons (e.g., Sternberg & Dalgarno 1989). The photodissociation region (PDR) associated with NGC 7023 has been studied extensively at radio (Fuente et al. 1990, 1992, 1993, 1996; Rogers, Heyer, & Dewdney 1995), infrared (Lemaire et al. 1996), and ultraviolet wavelengths (e.g., Witt et al. 1992, 1993; Murthy et al. 1993). Rogers et al. (1995) analyzed H I and ^{13}CO emission in order to describe the transition from atomic to molecular hydrogen. They used the correspondence between ^{13}CO emission and H_2 for dark clouds (Dickman 1978) to estimate the distribution of H_2, and they concluded that the available models of PDRs do not reproduce the molecular distributions very well. Through observations of $^{13}C^{16}O$ and $^{12}C^{18}O$ emission, Fuente et al. (1993) found that selective photodissociation of CO is occurring in NGC 7023; the more abundant isotopic variant shields itself more effectively than the rarer form does because the lines leading to photodissociation have larger optical depths. Fuente et al. also analyzed the distributions of CN and HCN and determined that the ratio of CN/HCN increases toward the illuminating source. The CN measurements at visible wavelengths that are described below are particularly relevant to these findings. At infrared wavelengths, Lemaire et al. (1996) studied H_2 emission from $v = 1$–0 $S(1)$ and $S(2)$ lines at high spatial resolution and detected high-density filaments. The peak brightness of the 1–0 $S(1)$ line is consistent with models invoking ultraviolet excitation followed by infrared decays. The main focus of the ultraviolet studies involved grain characteristics; the results are important ingredients for the analyses presented here.

Little attention, however, has been given to probing the line of sight to the illuminating star. Here we present results from high-resolution measurements of absorption from interstellar atoms and molecules toward HD 200775, the illuminating source of NGC 7023. The physical conditions for the gas are revealed through studies of the relative populations of rotational levels for C_2 (e.g., van Dishoeck & Black 1982; Lambert, Sheffer, & Federman 1995) and of the chemistry involving CH, C_2, and CN (e.g., Federman et al. 1994). These studies provide estimates for gas density and temperature and for the flux of dissociating ultraviolet radiation. Moreover, CH^+ and atomic absorption probe somewhat less dense gas (Cardelli, Federman, & Smith 1991), thereby yielding information on cloud structure along the line of sight. Such information for an infinitesimal pencil beam toward the illuminating source provides additional constraints for the models used in interpreting the radio and infrared data.

2. DATA ACQUISITION AND REDUCTION

We used two systems in our study of absorption from interstellar species at visible wavelengths: the coudé spectrograph on the 2.7 m telescope at McDonald Observatory and the coudé feed telescope at Kitt Peak National

[1] Guest Observer, McDonald Observatory, University of Texas at Austin.
[2] Visiting Astronomer, Kitt Peak National Observatory, National Optical Astronomy Observatories, which are operated by the Association of Universities for Research in Astronomy, Inc., under cooperative agreement with the National Science Foundation.

Observatory (KPNO). Three separate setups were employed in our high-resolution observations. At McDonald Observatory, during the period 1990–1992, single orders were imaged onto a Texas Instruments CCD with 15 μm pixels. Interference filters were used to block light from adjacent orders. Spectra were taken at four wavelength settings: CH^+ λ4232/Ca I λ4226, CH λ4300, Na I D, and K I λ7699. The spectral resolution, defined by the FWHM of lines from a Th-Ar hollow cathode lamp, was set at 2 km s^{-1}. The wavelength scale for the CH^+, Ca I, and CH measurements was defined by the Th-Ar spectra, and the scale was set by telluric features for the D lines (H_2O) and the K I line (O_2). Multiple exposures of HD 200775 were obtained in order to reach final signal-to-noise ratios of 50–100.

Multiorder spectra at a resolution of $\sim$3 km s^{-1} were acquired in 1993 at both sites. At McDonald Observatory, the "2dcoude" spectrograph on the 2.7 m telescope (Tull et al. 1995) was used to acquire spectra on interstellar C_2 at 8760 Å. The Texas Instruments CCD also served as the detector for these measurements. Since the C_2 lines are quite weak, multiple exposures were necessary, yielding a final signal-to-noise ratio of 600. At KPNO, the setup at the coudé feed telescope included Camera 5, an echelle grism, and the Texas Instruments No. 5 CCD. The nearly complete spectral coverage in the blue allowed us to search for absorption from CN near 3874 Å, Ca II H and K, CH $\lambda\lambda$3886, 4300, CH^+ $\lambda\lambda$3957, 4232, and Ca I λ4226. Summed spectra typically had signal-to-noise ratios of 50. For both runs, the spectral resolution and wavelength scale were determined by lines from a Th-Ar comparison lamp.

The raw images were reduced in the usual manner with IRAF procedures. Dark and bias frames were subtracted from each stellar image and flat-field frame. Cosmic-ray hits and scattered light were removed from each stellar image and flat field. The flat fields were divided into the stellar images to account for differences in pixel-to-pixel sensitivity. For orders containing interstellar features, pixels perpendicular to the dispersion axis were summed. The wavelength scales were set by Th-Ar comparison spectra that were taken several times each night. After correcting for Doppler motion, individual spectra taken throughout a run were combined. The combined spectra were normalized to unity and were used to measure the amount of interstellar absorption. The final spectra showing interstellar absorption appear in Figures 1, 2, and 3.

The equivalent width, W_λ, for a line was determined by a Gaussian fit; single Gaussians were adequate for all but the Na I D and K I lines. These fits also yielded an estimate of the Doppler parameter from the line's FWHM, corrected for instrumental width. Each W_λ was converted into a column density utilizing curves of growth. Doppler parameters (b-values) were set at 1 km s^{-1} for all lines except those of CH^+ and Ca II, where a b-value of 2.5 km s^{-1} was used, and those for the bluest component(s) of Na I D, where the doublet ratio method (Münch 1968) with a ratio of 1.5 was used. These values are consistent with results of ultrahigh-resolution measurements of similar sight lines (e.g., Crane, Lambert, & Sheffer 1995; Crawford 1995). The oscillator strengths needed for the conversion into atomic column densities were taken from Morton (1991); the molecular data noted in our earlier papers (e.g., Federman et al. 1994) were adopted here.

Table 1 lists our results acquired at blue wavelengths, and Table 2 displays the results for C_2. In Table 1, the results on v_{LSR}, W_λ, and the b-value for the data acquired at KPNO and McDonald Observatory are presented. In addition, the W_λ of CH λ4300 taken at moderate spectral resolution (Federman et al. 1994) and the derived column densities are shown. There are several points to note about the table listings. First, the data from different telescopes yield consis-

TABLE 1

COMPILATION OF RESULTS FOR HD 200775

	KPNO			McDONALD			FEDERMAN ET AL. 1994	
LINE	v_{LSR} (km s^{-1})	W_λ (mÅ)	b (km s^{-1})	v_{LSR} (km s^{-1})	W_λ (mÅ)	b (km s^{-1})	W_λ (mÅ)	N (cm^{-2})
Na I D_1	...	...	...	−3.7	92.4 ± 1.8	3.3	...	$(1.2 \pm 0.2) \times 10^{12}$
	...	...	...	−0.9	51.8 ± 1.1	1.7	...	$(1.4 \pm 0.1) \times 10^{12}$
	...	...	...	+2.2	64.8 ± 1.1	1.8	...	$(3.3 \pm 0.3) \times 10^{12}$
N_T(Na I)	...	...	...	...	...	...	...	$(5.9 \pm 0.8) \times 10^{12}$
K I	...	...	...	−2.0	4.5 ± 0.6	0.9	...	$(2.6 \pm 0.4) \times 10^{10}$
	...	...	...	−0.2	9.5 ± 0.5	0.3	...	$(5.8 \pm 0.3) \times 10^{10}$
	...	...	...	+1.7	4.6 ± 0.5	0.4	...	$(2.7 \pm 0.3) \times 10^{10}$
N_T(K I)	...	...	...	...	...	...	...	$(1.1 \pm 0.1) \times 10^{11}$
Ca II K	−2.7	80.5 ± 3.5	5.3[a]	...	...	...	...	$(2.2 \pm 0.3) \times 10^{12}$
Ca II H	−0.5	45.1 ± 2.8	4.9[a]	...	...	...	...	$(1.5 \pm 0.1) \times 10^{12}$
Ca I	...	≤7.2	...	...	≤3.9	...	...	$\leq 1.7 \times 10^{10}$
CH λ4300	+1.5	18.5 ± 1.4	2.7	+1.0	17.1 ± 2.0	2.0	23.4 ± 2.5	$(3.2 \pm 0.2) \times 10^{13}$[b]
CH λ3886	+1.9	5.5 ± 1.2	1.0	...	...	...	...	$(2.7 \pm 0.7) \times 10^{13}$[c]
N_T(CH)	...	...	...	...	...	...	...	$(3.2 \pm 0.2) \times 10^{13}$
CH^+ λ4232.....	−2.1	7.5 ± 1.1	2.3	−1.0	7.7 ± 1.3	1.9	...	$(9.1 \pm 1.0) \times 10^{12}$[b]
CH^+ λ3957.....	−0.6	4.4 ± 0.8	2.6	...	...	...	...	$(9.9 \pm 1.8) \times 10^{12}$
$N_T(CH^+)$	...	...	...	...	...	...	...	$(9.3 \pm 0.9) \times 10^{12}$
CN $R(0)$	+1.0	22.2 ± 1.7	2.5	...	...	...	...	$(7.9 \pm 1.0) \times 10^{12}$
CN $R(1)$	+1.3	10.5 ± 1.6	2.3	...	...	...	...	$(4.2 \pm 0.8) \times 10^{12}$
CN $P(1)$	+0.8	5.2 ± 1.5	1.4	...	...	...	...	$(3.7 \pm 1.2) \times 10^{12}$
N_T(CN)[d]	...	...	...	...	...	...	...	$(1.2 \pm 0.1) \times 10^{13}$

[a] The Ca II lines are especially broad, probably indicating blends. This could cause the difference in N from the H and K lines.

[b] Column density from weighted mean of measurements.

[c] The column density was multiplied by 2 because only one of 2 levels was analyzed, but equal populations were assumed.

[d] Total column density based on weighted average for $N = 1$. T_{ex} lies between 2.6 and 3.7 K.

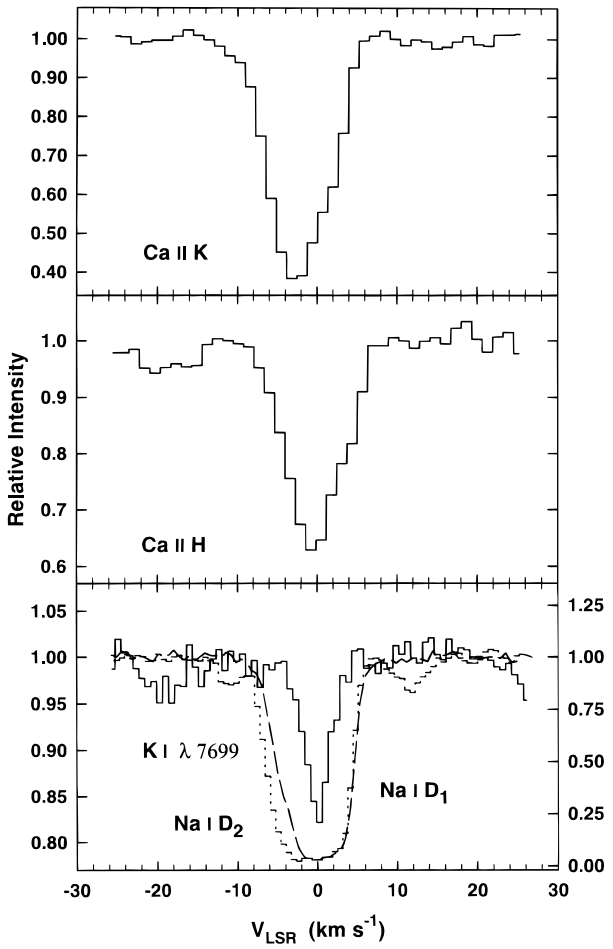

FIG. 1.—Spectra showing absorption from atomic species. The lowest panel displays K I λ7699 as a solid line, Na I D_1 as a long-dashed line, and Na I D_2 as a short-dashed line. Note that the red sides of the D lines overlap, indicating a doublet ratio near 1, while the blue sides show more absorption from D_2. For the blue component(s), a ratio of 1.5 is more appropriate.

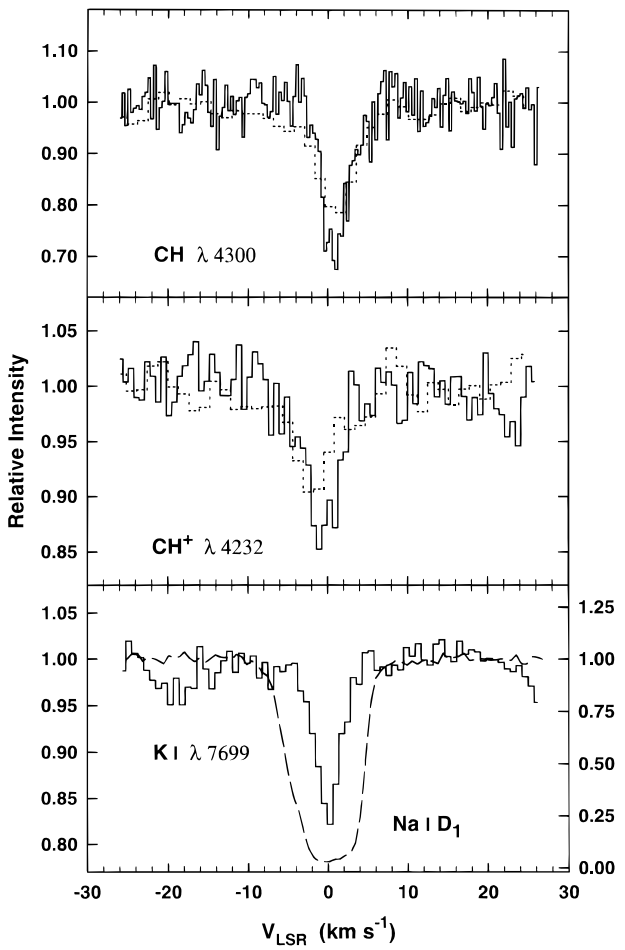

FIG. 2.—Spectra showing absorption from CH and CH^+ and from neutral Na and K. For the molecular absorption, the solid lines are from data taken at McDonald Observatory, and the dotted lines are the data from KPNO. Since the McDonald observations were acquired at higher resolution, the CH and CH^+ lines are deeper for these measurements.

tent values of v_{LSR}, W_λ, and b for CH λ4300, CH^+ λ4232, and Ca I λ4226. The column densities listed in the last column are based on weighted averages of the available measurements. Second, the two lines for CH, CH^+, and CN

TABLE 2

C_2 RESULTS

Line	v_{LSR} (km s^{-1})	W_λ (mÅ)	b (km s^{-1})	N (cm^{-2})
$R(0)$	−1.4	1.09 (0.27)	3.0	$(1.61 \pm 0.40) \times 10^{12}$
$N(0)$	...	...	...	$(1.61 \pm 0.40) \times 10^{12}$
$R(2)$	+2.2	0.95 (0.21)	0.6	$(3.53 \pm 0.79) \times 10^{12}$
$Q(2)$	...	...	...	...
$N(2)$	...	...	...	$(3.53 \pm 0.79) \times 10^{12}$
$R(4)$	...	≤0.41	...	$\leq 1.80 \times 10^{12}$
$Q(4)$	−0.3	0.70 (0.22)	2.1	$(2.07 \pm 0.65) \times 10^{12}$
$N(4)$	...	...	...	$(2.07 \pm 0.65) \times 10^{12}$
$R(6)$	...	≤0.41	...	$\leq 1.95 \times 10^{12}$
$Q(6)$	−1.8	0.69 (0.19)	2.4	$(2.03 \pm 0.56) \times 10^{12}$
$N(6)$	...	...	...	$(2.03 \pm 0.56) \times 10^{12}$
$Q(8)$	...	≤0.42	...	$\leq 1.23 \times 10^{12}$
$N(8)$	...	...	...	$\leq 1.23 \times 10^{12}$
$N(10)$[a].....	...	...	...	9.84×10^{11}
N_{tot}[b]	...	...	...	1.18×10^{13}

[a] An estimate.

[b] Based on estimates for $N(8)$ and $N(10)$.

($N = 1$) give comparable column densities; the total column densities used in our analysis are a weighted average of these determinations. Third, the results for the H and K lines of Ca II should give the same Ca II column density, but this may not be the case here. Unfortunately, the spectral resolution of the KPNO data is not high enough to discern multiple components in either line.

As for the C_2 results given in Table 2, the differences in velocity are probably caused by the weakness of the absorption. Although only one line was detected for each rotational level, the upper limits on $R(4)$ and $R(6)$ are consistent with the detected Q lines. The derivation of the total column density of C_2 included contributions from the levels $J = 8$ and 10, as shown in the table. These contributions were obtained from an excitation temperature $T_{ex} = T_{4,6}$ of 150 K (see Fig. 4).

The blue data reveal some interesting trends in radial velocity. (The C_2 lines are too weak for precise information about velocity.) The CH and CN lines have v_{LSR} of 1–2 km s^{-1}, and a component of Na I and K I is found at this velocity. This velocity agrees with that for the molecular cloud associated with NGC 7023, as revealed by radio emission lines (Feunte et al. 1990, 1993; Rogers et al. 1995). The neutral atomic lines also have components at ~ -1 and ~ -3 km s^{-1}. The CH^+ lines appear to be associated with

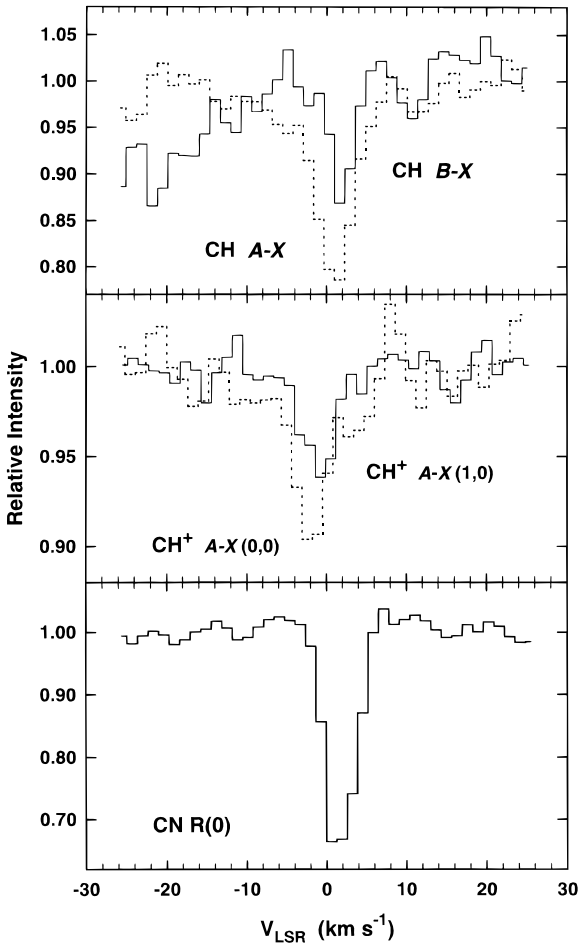

FIG. 3.—Spectra taken at KPNO showing absorption from CH, CH^+, and CN. For CH and CH^+ absorption, the solid lines are of the CH B–X (0, 0) and CH^+ A–X (1, 0) bands; the dotted lines are of the A–X (0, 0) band for both molecules. The results for each band yield similar column densities (see Table 1), and therefore the presence of differing strengths for the CH and CH^+ lines arises solely from different oscillator strengths. In the upper panel, the sloping continuum for the CH B–X transition is due to a stellar feature.

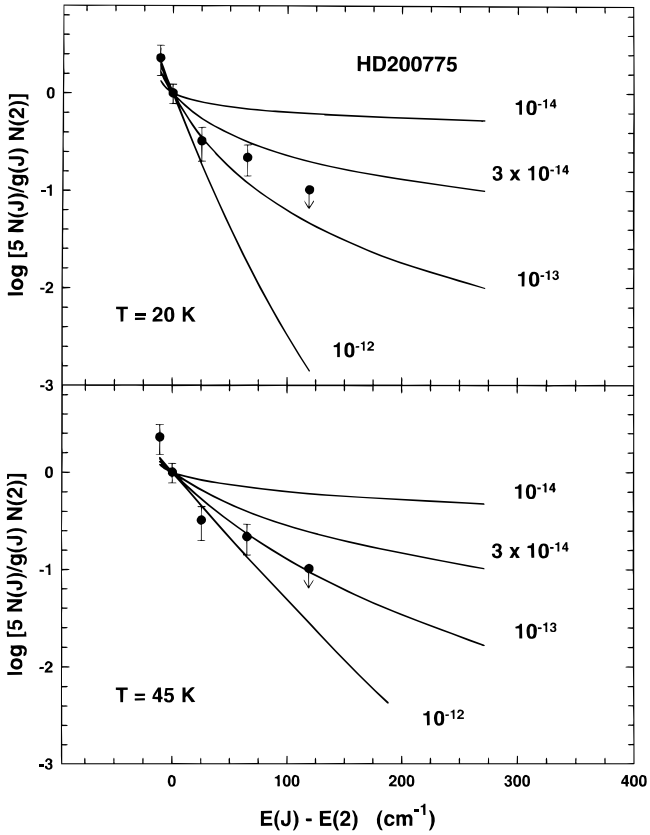

FIG. 4.—Excitation analysis for C_2. The theoretical results (van Dishoeck & Black 1982) are shown for two kinetic temperatures—20 and 45 K—along with the data (*filled circles with error bars*). The labels for the theoretical curves indicate the value for $n_c\sigma/I_{ir}$.

the component at -1 km s^{-1}. Since the Ca II lines appear at negative velocities only, calcium is not associated with the neutral/molecular component; instead, it is severely depleted onto dust grains, a finding consistent with the conclusions of Crinklaw, Federman, & Joseph (1994). The differences in velocity for the H and K lines may be caused by unresolved structure: the stronger K line shows significant absorption from the bluest component. A comparison of Figures 1, 2, and 3 reveals the differences in velocity structure among probes.

3. ANALYSIS AND RESULTS

3.1. *Molecular Excitation and Abundances*

The physical conditions in the gas can be derived from analyses of molecular excitation and synthesis (e.g., van Dishoeck & Black 1986; Federman et al. 1994). The conditions of most interest to us are gas density and temperature and the flux of ultraviolet radiation permeating the PDR in front of the star. The main observables are the relative populations of rotational levels in C_2 and the column densities of C_2 and CN. The goal is to model the excitation of C_2 (van Dishoeck & Black 1982) and to fit the C_2 and CN column densities by using a network of gas-phase reactions. [In principle, the excitation of CN may be used too (Black & van Dishoeck 1991). However, here the excitation temperature for CN is found to lie between 2.6 and 3.7 K, which, unfortunately, is indistinguishable from the temperature associated with the cosmic background radiation, and thus no information on physical conditions could be extracted from T_{ex}(CN).]

The distribution of C_2 rotational levels is shown in Figure 4, a plot of the population in level J relative to the amount in $J = 2$ versus energy of the level in units of cm^{-1}. The data are displayed with theoretical predictions for excitation (van Dishoeck & Black 1982) at two kinetic temperatures for the gas, namely, 20 and 45 K. The various curves represent the distributions expected for different values of $n_c\sigma/I_{ir}$, where n_c is the density of colliding partners, $n(H) + n(H_2)$, σ is the cross section for collisional deexcitation, and I_{ir} is the enhancement in the flux of infrared radiation over the interstellar value. (The high-lying rotational levels can be populated through collisions and photon pumping. The latter process involves absorption of infrared photons, leading to transitions between the ground vibrational level and the first excited electronic state, followed by radiative decays that return the molecules to various vibrational levels in the ground electronic state and finally radiative cascades to the ground vibrational level.)

The C_2 data displayed in Figure 4 are most consistent with the theoretical predictions for kinetic temperatures between 20 and 45 K. The measurement of the $R(0)$ line is not crossed by any of the theoretical predictions for $T = 45$

K, thereby setting the upper bound. Our upper limit for absorption from the $J = 8$ level places constraints on the value for $n_c \sigma / I_{ir}$; in particular, the value must lie above 6×10^{-14}. Appropriate maximum values are 2×10^{-13} for 20 K and 1×10^{-12} for 45 K. By using a value of 2×10^{-16} cm^2 for the de-excitation cross section (van Dishoeck & Black 1982) and setting I_{ir} equal to 1.0, we find that n_c lies between 300 and 550 cm^{-3} when we incorporate the factor of 1.8 reduction noted by van Dishoeck & Black (1982). For comparison with the chemical results, the density of hydrogen nuclei in all forms, $n(H) + 2n(H_2)$, is needed. Since $n(H) \approx n(H_2)$, this density is about 50% larger than n_c in diffuse gas, and therefore we derive a value for the gas density, n, of 450–800 cm^{-3}. In light of recent developments concerning C_2, these results may require some revision (see § 4).

Another means of extracting density, temperature, and radiative flux involves analysis of molecular production. Here we follow the analysis of Federman et al. (1994) for C_2 and CN chemistry; the reaction rate coefficients and photodissociation rates are the same as those in our earlier work. The basic rate equations, in terms of column densities, are

$$N(C_2) = \frac{k_1 x(C^+) \alpha n N(CH)}{G(C_2) + k_2 x(O) n + k_3 x(N) n}, \quad (1)$$

$$N(CN) = \frac{[k_3 x(N) N(C_2) + k_4 x(N) N(CH) + k_5 x(C^+) \alpha N(NH)] n}{G(CN) + k_6 x(O) n}. \quad (2)$$

In these equations, $N(X)$ and $x(X)$ are the column density and fractional abundance relative to the total number of protons for species X, k_i is the rate coefficient for reaction i, and $G(X)$ is the photodissociation rate that includes the effects of grain extinction. The parameter α provides a way to estimate the amount of C^+ converted into neutral atoms and CO (see Federman & Huntress 1989). As noted in Federman et al. (1994), α is a function of τ_{uv}, the grain extinction at far-ultraviolet wavelengths. For the sight line toward HD 200775, τ_{uv} was set at 4.05, a value that takes into account the rapid increase in extinction at short wavelengths (Walker et al. 1980; Buss et al. 1994). As for the column density for NH, it was estimated by scaling the results of Meyer & Roth (1991) for the gas toward ζ Persei by the ratio of CH columns.

The chemical analysis resulted in constraints on the acceptable values for n, T, and I_{uv}, where I_{uv} is the enhancement in the local ultraviolet flux over the average interstellar flux (e.g., Draine 1978). We used the observed $N(CH)$ (3.2×10^{13} cm^{-2}) and $N(C_2)$ (1.2×10^{13} cm^{-2}) in deriving the expected columns of C_2 and CN. Since variations in T had little effect on the outcome, T was set at 30 K. For C_2, we derived a column density of $\sim 1.3 \times 10^{13}$ cm^{-2} for densities between 150 and 500 cm^{-3} and values for I_{uv} of 1 and 3, respectively. The fact that the predicted value for $N(C_2)$ is not dependent on n/I_{uv} indicates that photodissociation is the dominant destruction process. This is not surprising for gas associated with a PDR. These values for n and I_{uv} lead to a value for $N(CN)$ of $\sim 2.5 \times 10^{12}$ cm^{-2}, which is significantly less than our measured value of 1.2×10^{13} cm^{-2}. We could not find any combination of parameters that reproduced both observed column densities in a satisfactory manner. The situation is reminiscent of the case of HD 29647, whose sight line probes material in TMC-1 (e.g., Federman et al. 1994). Federman et al. surmised that a contribution to CN production from dark cloud chemical schemes was necessary; this conclusion seems to apply to the gas toward HD 200775 also. Fuente et al. (1993), based on their radio observations, saw an increase in the ratio of CN/HCN toward the star. The radio emission lines come from the molecular cloud being dissociated by HD 200775. This point, as well as the differences in the derived parameters from the two analyses—excitation and chemistry—described here, is treated in more detail in § 4.

3.2. *Neutral Atoms*

The Na I and K I absorption arises from a minor ionization stage for the elements Na and K; the most abundant ions are Na II and K II. This fact simplifies the analysis based on ionization balance. The column density of neutral species X is given by

$$N(X) = \frac{N_{tot}(H) A(X) \alpha(X) n_e}{G(X)}. \quad (3)$$

In this expression, $N_{tot}(H)$ is the total proton column density, $N(H\ I) + 2N(H_2)$, $A(X)$ is the elemental abundance (Anders & Grevesse 1989), $\alpha(X)$ is the radiative recombination rate constant (Péquinot & Aldrovandi 1986), and n_e is electron density. The factor $A(X)$ includes depletion onto grains, which, for alkalis, is about a factor of 0.25 (Phillips, Pettini, & Gondhalekar 1984). The photoionization rates for Na I and K I are based on the measured ionization cross sections of Hudson & Carter (1967a) and of Hudson & Carter (1965, 1967b), Marr & Creek (1968), and Sandner et al. (1981), on the radiation field of Draine (1978), and on the grain extinction derived by Walker et al. (1980) and Buss et al. (1994). Many of the uncertain parameters in equation (3) can be eliminated when the ratio for N(Na I) to N(K I) is considered. This ratio can be written as

$$\frac{N(Na\ I)}{N(K\ I)} = \left[\frac{A(Na)}{A(K)}\right]\left[\frac{\alpha(Na\ I)}{\alpha(K\ I)}\right]\left[\frac{G(K\ I)}{G(Na\ I)}\right], \quad (4)$$

where $A(Na)/A(K)$ is 16 and $\alpha(Na\ I)/\alpha(K\ I)$ is 0.95.

Before analyzing the atomic absorption toward HD 200775, where the sight line has a nontypical extinction curve, we checked the validity of our expressions by examining the results for ζ Per. Curves of growth for the Na I doublet at 3302 Å (data from Crutcher 1975) and for K I λ7699 (Hobbs 1974) yield respective column densities of $(1.1 \pm 0.1) \times 10^{14}$ cm^{-2} and $(1.8 \pm 0.2) \times 10^{12}$ cm^{-2}. (A b-value of 1 km s^{-1} was adopted here as well.) The value for τ_{uv} over the wavelength interval 912–2500 Å is ≈ 1.7 when the extinction curve of Code et al. (1976) and forward scattering is considered. For this optical depth, the photoionization rates for Na I and K I are 4.5×10^{-12} s^{-1} and 1.5×10^{-11} s^{-1}, respectively. The predicted ratio for $N(Na\ I)/N(K\ I)$ is 51, which is similar to the observed ratio of 61 ± 9.

The extinction curve for the sight line to HD 200775 is lower than a typical one above 1200 Å, but it is above the typical one at shorter wavelengths (Walker et al. 1980; Buss et al. 1994). The average differences in optical depth suggest that the photoionization rates above 1200 Å need to be multiplied by 10, while at shorter wavelengths, the multiplicative factor is 0.25. These differences translate into Na I

and K I photoionization rates of 3.4×10^{-11} s^{-1} and 1.1×10^{-10} s^{-1}, respectively. We note that although there is more far-ultraviolet extinction, and hence smaller molecular photodestruction rates, toward HD 200775, the photoionization rates are larger than typical ones because the extinction is below the typical extinction curve over a larger wavelength interval. The larger amounts of photoionization lead to smaller columns of neutral atoms, as is observed to be the case (see following paragraph and Table 1). The predicted column density ratio becomes 49 and agrees nicely with the observed ratio of 54 ± 9 toward HD 200775. The good correspondences between the predicted and observed ratios indicate that equation (4), with the adopted photoionization rates, is a fair representation for the line of sight.

A more insightful comparison involves the predictions for the ratio in column densities for a specific atom for the sight lines toward ζ Per and HD 200775. This comparison allows us to probe potential differences in depletion onto grains and electron density, n_e (see eq. [3]). The total proton column densities are needed for this comparison. For the direction toward ζ Per, Savage et al. (1977) give $N_{\rm tot}({\rm H}) = 1.6 \times 10^{21}$ cm^{-2}, and for the sight line toward HD 200775, we use $N_{\rm tot}({\rm H}) = (2.3 \pm 0.3) \times 10^{21}$ cm^{-2}, which is based on the independent analyses of Witt & Cottrell (1980) and Buss et al. (1994). The values for n, T, and $I_{\rm uv}$ toward ζ Per—700 cm^{-3}, 30 K, and 1—are from the analyses of Federman et al. (1994). The chemical results presented above are used for the gas toward HD 200775. With this information, the predicted ratios (HD 200775/ζ Per) are the same for the two neutral species, 0.04 ± 0.01. These predictions agree very nicely with the observed ratios of 0.05 ± 0.1 and 0.06 ± 0.01 for Na I and K I, respectively.

4. DISCUSSION

Our analyses rely on a number of parameters, some of which are not well known. Here we consider the effects these have on our conclusions. In particular, we discuss the changes resulting from different oscillator strengths for the A–X transition in C_2, from different collisional de-excitation cross sections for C_2, from the fact that $I_{\rm ir}$ need not be the same as $I_{\rm uv}$, and from variations in the electron density, n_e.

Until recently, two sets of band oscillator strengths for A–X transitions in C_2 were available. Experimental results for f_{20} yielded values of $\approx (1.0 \pm 0.1) \times 10^{-3}$ (Erman et al. 1982; Bauer et al. 1985), while a theoretical computation obtained $f_{20} = 1.44 \times 10^{-3}$ (Langhoff et al. 1990). We used the experimental f-value in deriving $N(C_2)$ and in the analysis of C_2 excitation. Additional astronomical and laboratory data now clarify the situation somewhat. In their analysis of absorption from the D–X (0, 0) band at 2313 Å, Lambert et al. (1995) inferred a value of $(1.23 \pm 0.16) \times 10^{-3}$ for f_{20} from a presumably accurate f-value for the D–X band and the amount of absorption in each band for the diffuse clouds toward ζ Oph. After accounting for nonradiative transitions between excited states in C_2, Erman & Iwamae (1995) obtained $f_{20} = (1.36 \pm 0.15) \times 10^{-3}$.

These recent determinations suggest a value of $\approx 1.3 \times 10^{-3}$ for the A–X (2, 0) band. A 30% increase in the f-value would lower our column density by a comparable amount because the C_2 lines are quite weak. However, a larger f-value would increase n, the total gas density derived from excitation, by a corresponding amount, yet the lower column density would suggest a decrease in the estimate for n from chemical considerations, thereby widening the gap between the two determinations. Since $N(C_2)$ is proportional to $n/I_{\rm uv}$, an enhanced flux of ultraviolet radiation would produce the same chemical effect. A change in either parameter, in conjunction with the lower value for $N(C_2)$, would lead to less CN production via diffuse cloud chemistry and would indicate a greater CN contribution from the molecular core (i.e., dark cloud chemistry). The changes described here also bear on earlier analyses, such as Federman et al. (1994); use of the revised f-value for C_2 would weaken the nice correspondences found in this earlier study.

A further complication involving C_2 excitation has to do with the appropriate set of collisional de-excitation cross sections. We adopted the cross section of van Dishoeck & Black (1982), yet Lavendy et al. (1991) and Robbe et al. (1992) obtained cross sections about a factor of 2 larger. Use of the larger cross sections would lower the estimate for n, in a sense compensating for the adoption of the larger oscillator strengths. As noted by Federman et al. (1994), consistent results involving C_2 excitation and the chemical scheme for C_2 and CN production are still possible by modifying several poorly known rate constants. However, the correspondences among density estimates from C_2, CN, and CO excitation would be worse.

The two estimates for gas density derived in § 3 can be made consistent by allowing the enhancement factors $I_{\rm ir}$ and $I_{\rm uv}$ to have different values. Since the extinction curve for the sight line to HD 200775 is lower than a typical curve at wavelengths beyond 1200 Å and higher at shorter wavelengths, different values are very likely. These differences were noted above in the discussion of photodissociation and photoionization rates. Less extinction than is typical at long wavelengths leads to a value for $I_{\rm ir}$ that is larger than the value for $I_{\rm uv}$. In particular, consistent results (with the original f-values and cross sections) are possible with $I_{\rm ir}$ of about 3 or 4. Then the n estimate becomes 100–200 cm^{-3}, which compares with $150 I_{\rm uv}$ cm^{-3} from the chemical analysis. If $I_{\rm uv}$ were greater than 1, $I_{\rm ir}$ would have to be increased accordingly. We can conclude from this discussion that the gas density is probably known to within a factor or 2.

The values for $I_{\rm uv}$ and $I_{\rm ir}$ can be used to estimate the distance that the foreground material, probed by our observations, is from the star. Buss et al. (1994) measured a flux at 1050 Å of 5×10^{-13} ergs cm^{-2} s^{-1} Å^{-1} for HD 200775. With an interstellar flux of 2.65×10^{-6} ergs cm^{-2} s^{-1} Å^{-1} (about 50% larger than the value from Draine 1978) and a distance to the star of 600 pc (Hillenbrand et al. 1992), we derive a range of 1–2 pc for the distance between gas and star. This range is based on an optical depth of 4 for grain extinction in the foreground material. Similarly, the use of $I = 6.35$ and $J = 6.10$ for HD 200775 (Hillenbrand et al. 1992), corrected for extinction, and the interstellar infrared flux (see van Dishoeck & Black 1982) yields a distance of ~ 1 pc.

These distance estimates are consistent with results from H_2 infrared emission. In particular, Martini, Sellgren, & Hora (1997) suggested that the infrared emission arose from absorption of ultraviolet photons with a flux 10^3–10^4 times the average interstellar value. The H_2 emission comes from filaments approximately 0.1–0.2 pc from HD 200775. Our results indicate that the flux at 0.1–0.2 pc from the star is 300–1200 times the average interstellar flux.

A worthwhile comparison involves our derived gas density for the material in front of HD 200775 with other determinations. Witt & Cottrell (1980) obtained a value of ~ 245 cm^{-3} from their estimate for $E(B-V)$ of 0.44 mag, the ratio of $N_{\rm tot}({\rm H})/E(B-V)$ (Bohlin, Savage, & Drake 1978), and an estimate for the extent of the material in front of the star. Witt et al. (1982) found an average density of 400 cm^{-3} from the amount of ultraviolet scattering by dust; they suggested that the density varied from about 300 cm^{-3} near the edge of the nebula to 500 cm^{-3} near the star. The agreement between our results and those of A. N. Witt and colleagues is reassuring in light of the uncertainties noted above for our analysis and in the estimate of Witt et al. (1982) for the extent of the foreground material. Furthermore, Rogers et al. (1995) used H I 21 cm emission to derive an average density of 34 cm^{-3}; this lower estimate is not unexpected because inclusion of the purely atomic gas (Na I, K I, and Ca II) seen at negative velocities would lower the estimate for density.

Analysis of radio emission lines yields a density for the molecular cloud associated with NGC 7023. Elmegreen & Elmegreen (1978) derived a value of 600 cm^{-3} by using ^{13}CO measurements with the conversion factor to H_2 column density of Dickman (1978). Similarly, Watt et al. (1986) found a density of 860 cm^{-3} for interclump gas and 5.3×10^4 cm^{-3} in a dense clump. The far-infrared lines of O I and C II arising from the PDR (Chokshi et al. 1988) indicate a density of 4.4×10^3 cm^{-3}. Rogers et al. (1995) found densities of $\sim 10^4$ cm^{-3} in clumps within the molecular cavity (PDR). Their estimate was based on C^{18}O observations and the conversion factor to $N(H_2)$ of Frerking, Langer, & Wilson (1982). They also determined the peak density within the PDR from H I emission, obtaining a value of about 2.3×10^3 cm^{-3} that is consistent with other probes of the PDR (e.g., Chokshi et al. 1988). Most recently, Fuente et al. (1996), who analyzed emission from HCO^+, obtained densities of a few 10^5 cm^{-3} in the filaments associated with H_2 emission at infrared wavelengths (Lemaire et al. 1996). As expected, the radio emission lines probe the more dense, *primarily* molecular gas behind the star.

Although the correspondence between the Na I and K I results for HD 200775 relative to those for ζ Per is quite good, it is somewhat surprising that no differences in depletion level or ionization fraction ($x_e = n_e/n$) are needed to explain the observed ratios. Since $N_{\rm tot}$(H) is similar along the two sight lines, there may be little differential depletion to consider. The chemical results for the gas toward HD 200775 are based on a reduction in the abundance of C^+, the main contributor to x_e in diffuse gas. The abundance of C^+ is predicted to be only 15% of that toward ζ Per. A possible cause for the apparent inconsistency in the C^+ abundance is based on the fact that the atomic gas is more widely distributed than the molecular material. The existence of additional velocity components seen in the atomic absorption lines is one manifestation of this suggestion. The value for x_e is expected to be larger in the more widely dispersed "diffuse" atomic gas; our conclusion that the CN abundance indicates a contribution from the molecular core of the cloud is consistent with this premise.

The nebula's near-infrared emission includes the features called unidentified infrared bands (e.g., Cesarsky et al. 1996; Laureijs et al. 1996). The emission is attributed to very small grains and polycyclic aromatic hydrocarbons (PAHs). The PAH molecules may also be the source of the diffuse interstellar bands seen at visible wavelengths (see Snow et al. 1995), and they could affect the ionization balance in diffuse gas (Lepp et al. 1988). Snow et al. (1995) examined the suggestion that PAH^+ may be the carriers of the diffuse interstellar bands. Their analysis yielded the best conditions for a large abundance of PAH^+: a flux 10–100 times the average interstellar flux and a gas density of 100–1000 cm^{-3}. Our modeling efforts reveal that the radiation field permeating the foreground gas is much weaker than the necessary range, a conclusion consistent with the fact that the diffuse bands are weak or absent toward HD 200775 (see Snow et al. 1995). Lepp et al. (1988) modeled the effects of PAHs on the ionization balance in diffuse gas. Their results suggest that abundances are enhanced for neutral species with ionization potentials less than hydrogen's. Since we compared ratios in our analysis, the effects of including PAHs in the analysis should be minimal.

We detected an appreciable amount of CH^+ toward HD 200775. Its lines appear at bluer wavelengths than those of CH and CN (see Table 1). Since there are atomic components with similar velocities, the CH^+ absorption arises from primarily *atomic* gas. In terms of total column densities, the ratios $N(CH^+)/N(CH)$ and $N(CN)/N(CH)$ lie near the middle of the plot presented by Cardelli et al. (1990). A more meaningful comparison involves the CH associated with CH^+. The spectra shown in Figure 2 do not reveal any CH absorption above the noise at the velocity of the CH^+ line. The 2 σ limits for CH indicate that N(CH) is less than or equal to 4×10^{12} cm^{-2}, and the column of CH associated with CH^+ is $\leq 0.43N(CH^+)$, a value that is similar to the results for several other sight lines (see Federman, Welty, & Cardelli 1997). In other words, the CH^+ results for HD 200775 are not very different from those for other sight lines.

We were not able to reproduce simultaneously the amounts of C_2 and CN with our chemical schemes. It is likely that the "excess" amount of CN arises from dark cloud chemistry occurring in the molecular core, as previously inferred by Nercessian, Benayoun, & Viala (1988), van Dishoeck & Black (1989), and Federman et al. (1994) when modeling the material in front of HD 29647. This suggestion for the CN in the foreground material of NGC 7023 is consistent with maps obtained in radio lines of CN and HCN. Fuente et al. (1993) found an increase in the ratio of N(CN) to N(HCN) as they mapped material closer to HD 200775. Since the photodissociation rate for HCN is greater than the one for CN (van Dishoeck 1987), this result is not unexpected. We believe that the "excess" CN observed toward the star comes from the destruction of HCN, which is synthesized under the conditions found for the molecular cloud (see above).

5. FINAL REMARKS

We have presented the first chemical results for foreground material associated with the PDR in NGC 7023. Our main conclusions are that the kinetic temperature for the gas is ~ 30 K, that the gas density is ≈ 100–200 cm^{-3}, and that the flux of visible/infrared radiation is enhanced over the interstellar value and to a larger extent than the ultraviolet flux is, the last point being a consequence of the extinction curve for the line of sight. Our density estimates are similar to ones obtained from grain absorption and scattering in front of the star (Witt & Cottrell 1980; Witt et al. 1982). Uncertainties in our results arise because several

important parameters, including the C_2 de-excitation cross sections, are not well characterized. Effects associated with the background molecular cloud were also noted; these include severe depletion of Ca II in the velocity component associated with molecular gas and an enhanced abundance for CN from HCN photodissociation. The conditions associated with the molecular cloud ($n \sim 10^4$ cm^{-3}) are conducive for production of HCN. Our study of the lower density portion of the PDR provides additional constraints for models based on the radio and infrared data; these constraints include the acceptable range in density and temperature and the appropriate extinction law. Further improvements in our understanding of the lower density material are possible by combining the present analyses with results from diagnostics measured at far-ultraviolet wavelengths, such as neutral carbon, CO, and H_2. We are acquiring the necessary data through observations with the STIS on the *Hubble Space Telescope*. We will use the present results as a starting point in a refined, comprehensive modeling effort that incorporates the complete set of data.

This research was performed in part at the Jet Propulsion Laboratories, California Institute of Technology, under contract to the National Aeronautics and Space Administration. We thank John Black for his helpful suggestions.

REFERENCES

Anders, E., & Grevesse, N. 1989, Geochim. Cosmochim. Acta, 53, 197
Bauer, W., Becker, K. H., Hubrich, C., Meuser, R., & Wildt, J. 1985, ApJ, 296, 758
Black, J. H., & van Dishoeck, E. F. 1991, ApJ, 369, L9
Bohlin, R. C., Savage, B. D., & Drake, J. F. 1978, ApJ, 224, 132
Buss, R. H., Allen, M., McCandliss, S., Kruk, J., Liu, J.-C., & Brown, T. 1994, ApJ, 430, 630
Cardelli, J. A., Federman, S. R., & Smith, V. V. 1991, ApJ, 381, L17
Cardelli, J. A., Suntzeff, N. B., Edgar, R. J., & Savage, B. D. 1990, ApJ, 362, 551
Cesarsky, D., Lequeux, J., Abergel, A., Perault, M., Palazzi, E., Madden, S., & Tran, D. 1996, A&A, 315, L305
Chokshi, A., Tielens, A. G. G. M., Werner, M. W., & Castelaz, M. W. 1988, ApJ, 334, 803
Code, A. D., Davis, J., Bless, R. C., & Hanbury Brown, R. 1976, ApJ, 203, 417
Crane, P., Lambert, D. L., & Sheffer, Y. 1995, ApJS, 99, 107
Crawford, I. A. 1995, MNRAS, 277, 458
Crinklaw, G., Federman, S. R., & Joseph, C. L. 1994, ApJ, 424, 784
Crutcher, R. M. 1975, ApJ, 202, 634
Dickman, R. L. 1978, ApJS, 37, 407
Draine, B. T. 1978, ApJS, 36, 595
Elmegreen, D. M., & Elmegreen, B. G. 1978, ApJ, 220, 510
Erman, P., & Iwamae, A. 1995, ApJ, 450, L31
Erman, P., Larsson, M., Mannfors, B., & Lambert, D. L. 1982, ApJ, 253, 983
Federman, S. R., & Huntress, W. T. 1989, ApJ, 338, 140
Federman, S. R., Strom, C. J., Lambert, D. L., Cardelli, J. A., Smith, V. V., & Joseph, C. L. 1994, ApJ, 424, 772
Federman, S. R., Welty, D. E., & Cardelli, J. A. 1997, ApJ, 481, 795
Frerking, M. A., Langer, W. D., & Wilson, R. W. 1982, ApJ, 262, 590
Fuente, A., Martín-Pintado, J., Cernicharo, J., & Bachiller, R. 1990, A&A, 237, 471
———. 1993, A&A, 276, 473
Fuente, A., Martín-Pintado, J., Cernicharo, J., Brouillet, N., & Duvert, G. 1992, A&A, 260, 341
Fuente, A., Martín-Pintado, J., Neri, R., Rogers, C., & Moriarty-Schieven, G. 1996, A&A, 310, 286
Hillenbrand, L. A., Strom, S. E., Vrba, F. J., & Keene, J. 1992, ApJ, 397, 613
Hobbs, L. M. 1974, ApJ, 191, 381
Hudson, R. D., & Carter, V. L. 1965, Phys. Rev., 139, A1426
———. 1967a, J. Opt. Soc. Am., 57, 651
———. 1967b, J. Opt. Soc. Am., 57, 1471
Lambert, D. L., Sheffer, Y., & Federman, S. R. 1995, ApJ, 438, 740
Langhoff, S. R., Bauschlicher, C. W., Rendell, A. P., & Kormornicki, A. 1990, J. Chem. Phys., 92, 300
Laureijs, R. J., et al. 1996, A&A, 315, L313
Lavendy, H., Robbe, J. M., Chambaud, G., Levy, B., & Roueff, E. 1991, A&A, 251, 365
Lemaire, J. L., Field, D., Gerin, M., Leach, S., Pineau des Forêts, G., Rostas, F., & Rouan, D. 1996, A&A, 308, 895
Lepp, S., Dalgarno, A., van Dishoeck, E. F., & Black, J. H. 1988, ApJ, 329, 418
Marr, G. V., & Creek, D. M. 1968, Proc. R. Soc. London, A304, 233
Martini, P., Sellgren, K., & Hora, J. L. 1997, ApJ, 484, 296
Meyer, D. M., & Roth, K. C. 1991, ApJ, 376, L49
Morton, D. C. 1991, ApJS, 77, 119
Münch, G. 1968, in Nebulae & Interstellar Matter, ed. B. M. Middlehurst & L. H. Aller (Chicago: Univ. Chicago Press), 365
Murthy, J., Dring, A., Henry, R. C., Kruk, J. W., Blair, W. P., Kimble, R. A., & Durrance, S. T. 1993, ApJ, 408, L97
Nercessian, E., Benayoun, J. J., & Viala, Y. P. 1988, A&A, 195, 245
Péquignot, D., & Aldrovandi, S. M. V. 1986, A&A, 161, 169
Phillips, A. P., Pettini, M., & Gondhalekar, P. M. 1984, MNRAS, 206, 337
Robbe, J. M., Lavendy, H., Lemoine, D., & Pouilly, B. 1992, A&A, 256, 679
Rogers, C., Heyer, M. H., & Dewdney, P. E. 1995, ApJ, 442, 694
Sandner, W., Gallagher, T. F., Safinya, K. A., & Gounard, F. 1981, Phys. Rev., A23, 2732
Savage, B. D., Bohlin, R. C., Drake, J. F., & Budich, W. 1977, ApJ, 216, 291
Snow, T. P., Bakes, E. L. O., Buss, R. H., & Seab, C. G. 1995, A&A, 296, L37
Sternberg, A., & Dalgarno, A. 1989, ApJ, 338, 197
Tull, R. G., MacQueen, P. J., Sneden, C., & Lambert, D. L. 1995, PASP, 107, 251
van Dishoeck, E. F. 1987, in IAU Symp. 120, Astrochemistry, ed. M. S. Vardya & S. P. Tarafdar (Dordrecht: Reidel), 51
van Dishoeck, E. F., & Black, J. H. 1982, ApJ, 258, 533
———. 1986, ApJS, 62, 109
———. 1989, ApJ, 340, 273
Walker, G. A. H., Yang, S., Fahlmann, G. G., & Witt, A. N. 1980, PASP, 92, 411
Watt, G. D., Burton, W. B., Choe, S.-U., & Liszt, H. S. 1986, A&A, 163, 194
Witt, A. N., & Cottrell, M. J. 1980, ApJ, 235, 899
Witt, A. N., Petersohn, J. K., Bohlin, R.C., O'Connell, R. W., Roberts, M. S., Smith, A. M., & Stecher, T. P. 1992, ApJ, 395, L5
Witt, A. N., Petersohn, J. K., Holberg, J. B., Murthy, J., Dring, A., & Henry, R. C. 1993, ApJ, 410, 714
Witt, A. N., Walker, G. A. H., Bohlin, R. C., & Stecher, T. P. 1982, ApJ, 261, 492